Journal of Materials Chemistry B

Accepted Manuscript

ROYAL SOCIETY OF CHEMISTRY

www.rsc.org/materialsB

FITC/Suramin Harboring Silica Nanoformulations for Cellular and Embryonic Imaging/Anti-Angiogenic Theranostics

Srivani Veeranarayanan[1], Aby Cheruvathoor Poulose[1], M. Sheikh Mohamed[1], Yutaka Nagaoka[1], Shosaku Kashiwada[2], Toru Maekawa[1], D. Sakthi Kumar[1]

1. Bio Nano Electronics Research Centre, Graduate School of Interdisciplinary New Science, Toyo University, Kawagoe, Japan

2. Research Center for Life and Environmental Sciences, Toyo University, Itakura, Japan.

Corresponding author*

Prof. D. Sakthi Kumar,

Ph: 81-492-39-1636

Fax: 81-492-34-2502

E-mail: sakthi@toyo.jp

Abstract

The *in vitro* and *in vivo* uptake, toxicological analysis and anti-angiogenic theranostic prospect of FITC loaded (FITC-Si) and suramin loaded (Sur-Si) silica nanoparticles is presented. FITC/suramin encapsulated silica nanoparticles (NPs) with an average size of □30 nm were synthesized. The uptake of FITC-Si by Human umbilical vein endothelial cells (HuVEC) (*in vitro*) and by early stage medaka embryos (*in vivo*) was monitored using fluorescence microscopy. The nanoformulation was found to be biocompatible to both cells as well embryos. The cytotoxicity analysis, tubulogenesis and migration assay confirmed the anti-angiogenic potential of Sur-Si NPs in HuVEC. The imaging of medaka embryos exposed to FITC-Si, their survival and hatching rate and biocompatibility post FITC-Si exposure were documented. The *in vivo* drug delivery mediated anti-angiogenic potential of Sur-Si NPs was assessed by survival and hatching rate analysis along with morphological indicators. At higher concentrations, Sur-Si proved lethal to embryos, whereas at lower concentrations was rather an efficient anti-angiogenic formulation leading to malformed vasculogenesis and inhibited intersegmental vessel formation in an efficient dose dependent mode. The results indicate the potential application of such a nanoformulation in future anti-angiogenic theranostics.

Keywords: Silica Nanoparticles, Theranostics, Medaka Embryos, Angiogenesis, Biocompatibility

1. Introduction

Nanoparticles have evolved into materials with immense value in mechanical, optical, electrical, magnetic and medical applications.[1-5] Theranostic nanoparticles for simultaneous imaging and therapeutic applications are currently gaining lot of attention for the treatment of a wide array of ailments. Application of such multifunctional nanomaterials and their prospective efficiencies are being testified at a stride never before with a huge repository of data accumulating in recent years.[6-9] Silica NPs exhibit certain advantages such as extended blood circulation times due to their hydrophilicity, versatile surface functionalization options, biocompatibility and ease of cost-effective large-scale synthesis. [10-12] Most of the recent reports on silica NPs have revolved around monodisperse 80 – 120 nm particles. However, not much research on the theranostic applications of non-porous silica NPs of size 20 - 50 nm is available. In terms of size, NPs between 20 – 50 nm are considered to be best suitable for *in vivo* theranostic applications as they can effectively escape reticulo-endothelial system (RES) clearance, lymphatic filtration as well kidney clearance, thereby facilitating longer circulation time. [13-15] Syntheses of porous silica NPs involves the use of toxic templates, which need to be later removed by acids. Also, the chances of cargo leak from these porous materials are a high possibility, requiring further capping to guard the cargo from getting released before reaching the intended target. As alternative non-porous silica, encapsulating bioactive agents in their oxide matrix with a size range of 20 – 50 nm would serve as an optimal theranostic platform to circumvent these limitations. Although most of the nanoparticle based therapeutic modules converge on cancer, prominence has been shifting towards modules that concentrate on other major patho-physiologies involved in the development of cancer.[16,17] Angiogenesis, an essential process in embryo-vascular development and regulation of crucial physiological processes, relates to the growth of new capillaries from pre-existing vessels. Disruption of angiogenesis can lead to pathologies such as unregulated vessel overgrowth, as in cancer, or vessel insufficiency, as in cardiovascular diseases. The importance of angiogenesis to tumor growth is such that, without the former, tumors stop to grow more than 2 mm in size.[18] Clinical research reports on breast cancer patients disclose the positive association between angiogenesis and the degree of metastasis, tumor recurrence and survival rates, underscoring the prominent role of this phenomenon as a prognostic cancer marker.[19]

Tumor angiogenesis and physiological angiogenesis share, to an extent, analogous sequence of events, though the former is unrestrained and excessive, leading to leaky and tortuous vasculature, credited to the over expression of growth factors and cytokines.[20] Noteworthy progress has been made to target and halt tumor angiogenesis to overpower tumor progression.[21] This has been made possible with a chemotherapy module in which drugs that either thwart the formation of new blood vessels supplying the tumor (e.g. TNP-470, endostatin, angiopoietin, vasostain), or impair existing ones (e.g. canstatin, angiostatin).[22] To achieve better efficacy, nanoparticles with anti-angiogenic drug loads have been formulated and targeted to regress angiogenic vessels in many *in vitro* and *in vivo* models.[23-25] The aim of the present investigation is to synthesize size tuned non-porous silica nanoparticles encapsulating a fluorescent dye, fluorescein isothiocyanate (FITC)/anti-angiogenic drug, suramin to determine nanoparticle uptake, translocation and drug effects thereof in HuVEC cells and medaka (*Oryzias latipes*) fish embryos. HuVEC was chosen as cellular model as they are of well-established endothelial lineages that are well known as *in vitro* angiogenesis model. Neo-angiogenesis resembles vasculogenesis in all aspects and therefore, fish vasculogenesis is considered to be a suitable model to study anti-angiogenic potential of various drug formulations because many anti-angiogenic drugs elicit similar responses in fish and mammalian systems alike.[26] Specifically, fish is an exciting vertebrate model for angiogenesis because of its substantial degree of genetic homology with humans. Moreover, they are amenable to direct intravital imaging with high spatial and temporal resolution through fluorescent tools. The embryo transparency is a valuable characteristic, and angiogenesis assays on medaka-fish embryos are very cooperative for pharmacological *in vivo* screening, since embryos can be maintained very easily.[27,28] In addition to the theranostics, we evaluated the potential toxicological risks of the nanoparticles by analyzing the embryonic development and hatching rate of the embryos. This work contributes to the environmental risk assessment of silica nanoparticles and also to the *in vivo* application of FITC and suramin nanoformulations for imaging guided anti-angiogenic therapy. Though numerous works on NP exposure to fish models have been performed, most have focused on the ecotoxicity aspects, however this report uses the nanoformulation to image and inhibit vasculogenesis in fish as a proof of concept for future anti-angiogenic cancer theranostics.

2. Materials and Methods

2.1 Materials

Aminopropyl trimethoxysilane (APTMS) and fluorescein isothiocyanate (FITC) were purchased from Aldrich. Tetraethyl orthosilicate (TEOS, 99%), Igepal (CO-520), methanol (anhydrous, 99.8%), acetone (p.a.), ammonia (25% in water, p.a.), dimethyl formamide (DMF) and ethanol (>99.8%) were purchased from Wako Chemicals. Human umbilical vein endothelial cells (HuVECs) were purchased from Gibco. Medium 200, LSGS, phosphate-buffered saline (PBS), trypsin, trypan blue and alamarBlue® were acquired from Invitrogen. Suramin sodium salt was purchased from Sigma. BD Matrigel was from BD Biosciences.

2.2 Synthesis of 30 nm FITC/Suramin loaded silica nanoparticles

Silica nanoparticles of size 30 nm were synthesized by microemulsion method.[29] FITC precursor solution was prepared by dissolving 0.5 mg in 1 ml DMF and 3-APTMS (12 mol % of TEOS) for 2 h in dark at room temperature with mild stirring. FITC incorporated silica nanoparticles were prepared by mixing cyclohexane and igepal CO-520 (at a ratio of 2.5:1) and were stirred until a transparent microemulsion was formed. Then 2 ml of TEOS and FITC precursor solution was added drop-by-drop and post which aqueous ammonia was added. The reaction is kept at RT and allowed to stir for 12 h. To prepare suramin loaded silica nanoparticles, same experimental procedure was followed except instead of FITC precursor solution, 1 mg/ml of suramin-ethanol solution was added directly to the microemulsion. The Si-NPs formed were precipitated using acetone. The precipitated product is repeatedly washed and desiccated to yield Si-NPs loaded with FITC/Suramin.

2.3 Nanoparticle characterization

The as-prepared NPs were characterized for their morphology using transmission electron microscopy, JEOL JEM-2200-FS (TEM). The photoluminescence measurements were done to analyze the FITC loading into the NPs using JASCO FP 6500 spectrofluorometer. The loading and release of drug, suramin was analyzed with UV-Vis spectrophotometer, Shimadzu UV-2100PC/3100PC UV visible spectrometer.

2.4 Cell culture and maintenance

HuVECs were maintained in T25 flasks using Medium 200 with low serum growth supplement. The cells were sub-cultured every 3 days. Cells were maintained in glass-base dishes and 96-well plates for confocal and cytotoxicity analysis, respectively. For cytotoxicity analysis, approximately 5000 cells were seeded into each of the 96-well plates. The cells were grown until visual confluence and were exposed to FITC-Si or Sur-Si NPs at varied concentrations (0.025 - 1 mg/mL). The control group was devoid of nanomaterials and the experiments were conducted in triplicate. After 72 hours of incubation with nanoparticles, the cells were washed with PBS and 0.1 mL of the respective medium was added. Cell viability was assayed with alamar blue according to the manufacturer's instruction. Confocal microscopy was carried out to analyze the entry of FITC-Si NPs into cellular cytosol. Approximately, 50,000 cells were plated onto glass-base dishes and cultured until 80% confluence. Subsequently, the FITC-Si NPs were added to the plates at a concentration of 100 μg/mL, and the cells were incubated for 2 hours at 37°C in an incubator maintained at 5% CO_2. The cells were then washed with PBS and viewed under a confocal microscope at 488 nm excitation with a green filter to visualize the effective imaging potential of the NPs. The migratory assay was conducted using cell culture inserts in 24-well plates. The cells (30,000 in number approximately) were plated onto the inserts and the inserts were immersed in 24-well plates with medium supplemented with the test substance, Sur-Si/FITC-Si NPs (concentration ranging from 0.025 – 1 mg/mL). The migratory nature of the cells was analyzed by trypan blue assay. Next, to investigate the *in vitro* tubulogenesis, HuVECs were plated onto 96-well plates pre-loaded with BD Matrigel matrix (100 μL). Sur-Si/FITC-Si NPs were added to the test wells at the concentration of 0.1 mg/mL. The plates were incubated for 4 h under ambient cell growth conditions and viewed by phase contrast microscopy for HuVECs' tube-forming ability in the presence and absence of Sur-Si/FITC-Si NPs.

2.5 Medaka fish culture and maintenance

Female and male medaka fish were cultured in 8 L aquarium tank. The breeding groups were fed with brine shrimp nauplii twice daily. The fish were maintained under 16/8 h light/dark cycle at 26ºC. Under this regular day night photoperiod ovulation occurs 1 h before the onset of light period. The fish used were treated

humanely in accordance with the institutional guidelines of Toyo University, with due consideration for the alleviation of distress and discomfort.

2.6 Embryo collections and sorting

Fresh medaka embryos were collected and the thin filaments holding the egg clusters together were removed by gently rolling the clusters between moistened papers. Thus gathered eggs were rinsed and placed in embryo rearing medium (ERM). The eggs were then sorted for viable and dead embryos and the former were directly utilized for nanoparticle exposure for imaging and anti-angiogenic therapy studies.

2.7 Nanoparticle exposure to the embryos

FITC-Si and Sur-Si NPs at concentrations of 50 µg/ml and 5 µg/ml (in ERM) were utilized to study particle exposure to the embryos. Both nanoparticles were weighed and added to ERM solution separately to obtain a well-dispersed solution. For this experiment, day 0 embryos (viable embryos collected on day of laying) were utilized. These fresh embryos were randomly selected for nanoparticle exposure (test group) and the experiment was carried out in 6 well plates. To each well, 15 embryos were placed and 2 ml of nanoparticle suspension was added. The experiments were set with duplicates. Hence, for each concentration of nanoparticle, 30 embryos were tested. The embryos were incubated at 25ºC till hatching under gentle shaking and were imaged for FITC-Si nanoparticle intake in due course using epi-fluorescence microscopy. The effect of FITC-Si on their morphology, embryonic development and hatching were analyzed. The control groups were also analyzed and imaged for comparison of embryonic development with test group. In the case of Sur-Si treated embryos, the embryos were analyzed for morphological malformation and vascular-disruption due to suramin.

2.8 Statistical analysis

All quantitative experiments were conducted with at least duplicate experiments. Statistical evaluation was performed and the analyzed data were expressed as mean ± Error Percentage.

3. Results and Discussion

3.1 Nanoparticle characterization

Size and shape tuned 30 nm silica nanoparticles were prepared via reverse-microemulsion method.[29] As shown in TEM micrographs (**Fig. 1a**), the FITC-Si NPs were of uniform spherical shape and size with high monodispersity. The PL spectra of FITC doped nano silica was obtained at excitation wavelength 365 nm and a clear emission peak was noted around 490–550 nm, typical for green fluorescein FITC, confirming successful loading of FITC into nano silica (**Fig. 1b**).

3.2 Suramin loading and release

The amount of suramin loaded into silica nanoparticles was quantified with the help of UV/Vis absorption spectroscopy by obtaining the absorption values of standard drug concentrations and correlating them. The encapsulation efficiency of suramin within silica nanoparticles was found to be 68 %. The release of suramin was studied using pH 7.4 PBS solution, appropriate for drug release studies owing to its similar ionic composition to human-body plasma. Suramin solutions of different concentrations were then prepared and measured to obtain standard curves. At different time intervals, the released drug was collected and centrifuged for analysis of the supernatant. The concentration of drug released in a given time was calculated by linear equation to determine the drug release curve. The nanoparticles showed sustained kinetics with nearly 72% release in 24 h. By 36 h, we found the release of drug to be saturated at 98 % depicting a complete release (**Fig. 2**). Drug release is proposed to be due to combination of diffusion of the encapsulated molecules and dissolution/degradation of silica over time in a biological/physiological system.[30]

3.3 Biocompatibility analysis of FITC-Silica NPs in vitro

To efficiently employ these nanomaterials as cellular imaging probes, imparting biocompatibility to them is of prime importance. As described, cytotoxicity tests were carried out using alamar blue on HuVECs. Upon subsequent addition of nanoparticles, cell viability decreased as a function of concentration and time. The population density/metabolic activity of viable HuVECs observed under different concentrations after 72 hour of nanoparticles incubation was studied (**Fig. 3**). At higher concentration (1 mg/mL) the viability was near to 80 %, which further increased (85 and 95 %) with subsequent decrease in nanoparticle concentration (0.5

and 0.1 mg/mL), respectively. At lower concentration, (0.05 and 0.025 mg/mL), the cells were 100 % viable. The high viability readings emphasize the prominent biocompatibility of these nanomaterials and their safe utilization in future cell/animal studies.

3.4 In vitro Imaging

HuVECs were treated with as few as 100 µg/mL of nanomaterials and incubated for 2 hour. Highly efficient endothelial labeling was observed with excellent uptake and internalization of the FITC-Si nanomaterials into the cell's cytosol (**Fig. 4**). FITC-silica NPs can be used as effective cell labels due to their cellular compatibility and proven enhanced photostability for extended periods of analysis.[21]

3.5 In vitro cytotoxicity of Sur-Si

To analyze therapeutic efficiency of the nanformulation; Sur-Si NPs were administered to cells. For this purpose, the toxicity rendered by these drug-loaded NPs was assessed. Suramin is a cytostatic drug that effectively disrupts cellular metabolism culminating in cell death regardless of the type or pathogenicity of the cells. It causes chromosomes to lose their telomeric end nucleotides by inhibiting telomerase, a ribonucleoprotein responsible for the elongation and/or maintainance of telomeres by TTAGGG tandem repeat sequence addition, utilizing the RNA component of the enzyme as a template. Enzyme activity appears to be associated with cell immortalization and malignant progression as telomerase activity has been found in the majority of human tumors and in angiogenic cells, but not in most somatic cells or tissues. The loss of telomeric ends by chromosomes eventually leads to cell death and telomerase inhibition has, therefore, been proposed as a novel and potential target for therapeutic intervention. As telomere loss causes senescence and apoptosis in cells treated with suramin, we employed the same in the form of a nanoformulation to achieve maximum effect. The Sur-Si NPs/Suramin were exposed to cells at different concentrations and post 72 h, the cytotoxicity was assayed by alamar blue to analyze the therapeutic proficiency of nanomaterials. HUVECs exposed to the positive control agent, Suramin at a concentration of 0.05 and 0.1 mg registered viability of 69 and 43 % respectively. The viability of HuVECs was

reduced to 10 % when exposed to 1 mg/mL Sur-silica NPs depicting the higher therapeutic efficiency, which was found to be dose dependent (**Fig. 5**)

3.6 Anti-angiogenic property in vitro

To assess the anti-angiogenic potential of Sur-Si NPs, migration and tube assays were performed. Migration assay was carried out to analyze the potential of HuVECs to migrate towards VEGF stimuli (a growth factor stimulant which induces angiogenesis). HuVECs were added to 3 μm pore cell culture inserts that were dipped into 24-well plates containing growth medium in the presence or absence of VEGF, FITC-silica and Sur-Si NPs and incubated for 24 h. The positive control experiment where HUVECs were exposed to Suramin at a concentration of 0.05 and 0.1 mg, registered 53 and 39 % cell migration. In spite of the presence of chemical stimulant, we did not observe any significant cell migration at the highest concentration of Sur-Si, whereas at the concentration of 100 μg/mL, 32 % cell migration was noted. This clearly depicts the antiangiogenic effects of Sur-Si formulation. However, with FITC-Si, HuVEC migration was witnessed which remained very much on par with the control group (**Fig. 6**).

Tube formation assay was also executed in the presence of FITC-Si and Sur-Si NPs. Typical tube formation ability of HuVECs was recorded by 4 h in controls and FITC-Si treated wells, whereas in the case of drug-loaded NP-treated cells, this inherent characteristic was totally diminished with the absence of any tube-like structures (**Fig. 7**). This emphatically projects the potential of the employed Sur-Si as potent anti-tumor and anti-angiogenic agent.

3.7 Biocompatibility of FITC-Si NPs to medaka embryos

Medaka embryos were treated with 2 different concentrations of FITC-Si NPs (50 and 5 μg/ml) until hatching (control group hatched on the 9^{th} day) to understand the biocompatibility and imaging potential of these nanoparticles *in vivo*. The viability of embryos and developmental embryonic malformations were recorded till hatching.

Survival rate

Figure 8 depicts the survival rate of medaka embryos treated with FITC-Si NPs. In the case of 50 μg/mL FITC-Si, all embryos were viable on day 2. 95 % of embryos

remained viable when analyzed on day 5 and on day 9, we observed 90 % of viable embryos. In the case of 5 µg/ml FITC-Si, all embryos were viable till day 9 of hatching and no morphological deformations of embryos or hatched larvae during the time under study was noted (from day 1 to day 15) suggesting that FITC-Si NPs were highly biocompatible with no intrinsic toxicity to embryos at both concentrations studied (See Supplementary Information File and Video for data on biocompatibility of FITC-Si NPs to Medaka embryos - Analysis of heart beat and blood flow).

Hatching rate

To analyze the effect of FITC-Si NPs on hatching rate, the embryos were incubated with previously mentioned two different concentrations of nanoparticles till the day control embryos hatched (day 9) (**Fig. 9**). All the control group embryos hatched on day 9, whereas in the case of 50 µg/ml FITC-Si treated embryos, 70 % got hatched on day 9, 20 % on day 10 and remaining hatched on day 11. This observation may be attributed to the aggregation of higher concentration of nanoparticles onto the embryo's chorionic membrane leading to lesser amount of transport of essential nutrients and gaseous exchange from surrounding medium to embryonic body. In the case of 5 µg/mL FITC-Si treated embryos, nearly 90 % embryos got hatched on day 9, remaining 10 % got hatched the day next. These results showed that FITC-Si nanoparticles do not possess any significant toxicity on survival, hatching and development of medaka embryos and could be employed safely in diverse *in vivo* applications.

3.8 Imaging of medaka embryos using FITC-Si NPs

To analyze whether FITC-Si nanoparticles can serve as highly biocompatible efficient imaging labels *in vivo*, we treated the embryos with the NPs and performed imaging studies on day 2, day 5 and day 10 to analyze the fluorescence from nanoprobe. The FITC-Si nanoparticles (50 and 5 µg/mL) were administered to embryos on day 1 until they hatched. In the case of 50 µg/mL FITC-Si (**Fig. 10**), the embryos, on day 2 showed aggregation of nanomaterial over the chorion's short villi. As a result, the entry of nanomaterial into embryos could not be analyzed because the fluorescent image showed higher nanoparticle aggregation on embryo surface making them appear opaque. Repeated rinsing of the embryos to remove the aggregated particles

was attempted but had no effect. The day 5 embryos showed less aggregation of nanoparticles on their outer membrane, but nanoparticle aggregation on the gill region of embryonic body was noticed. The fluorescent images also showed accumulation of nanoparticles in the anterior region (head) of embryonic body, evidenced by higher intensity of fluorescence from within this region, depicting the successful internalization of the nanomaterials. When the hatched larvae were analyzed, clear higher intensity fluorescence, especially from head region and in somites was visualized. In addition, there weren't any malformations as recorded from the bright field images of nanoparticle treated embryos, further proof of the excellent biocompatibility of these nanotools.

In the case of 5 μg/mL of FITC-Si treated embryos (**Fig. 11**), the nanoparticle entry at all stages under study could be observed and any particle aggregation on surface of embryos was seen, confirmed from the transparency of embryos. Particle internalization was recorded with bright fluorescence from the embryonic body from day 2 to day 9 until hatching, without any deformities or lethality. The nanoparticle entry could either be due to the lower aggregation or surface charge that aided in particle uptake through pore canal of embryos resulting in efficient *in vivo* imaging (See Supplementary Information File and Video for data on live fluorescence imaging of Medaka embryos that are exposed to FITC-Si NPs).

3.9 Anti-angiogenic effect of Sur-Si in medaka embryos

Suramin is considered to be a well-studied and best available anti-angiogenic drug; it can attack the endothelial progenitor cells and vascular progenitors, thereby leading to disrupted vasculogenesis *in vivo*, if entry into embryos is achieved. The disruption of vasculogenesis by this nanoformulation can be considered a success because vasculogenesis and angiogenesis are similar in molecular aspects and if targeted, this potent nanotool could be tailored to attack angiogenic cells alone in future.

50 μg/mL was chosen as test concentration for this study because at this concentration FITC-Si did not show any detrimental effects on embryos, establishing that this concentration of Si NPs was safe and reliable to study. At this concentration of Sur-Si, 50 % of embryos were viable till day 5, while all the embryos of this group were dead by day 9, due to the time dependent toxicity of suramin (**Fig. 12**). As none of the

embryos were alive by the end of the study, we couldn't observe any hatching (**Fig. 13**). Day 2 observations revealed rounded and shrunk embryonic bodies. Some embryos showed disruption of whole body leading to death. Embryos alive till day 5 showed formation of optic bud and the head, though a congested morphology and opaqueness (control embryonic body was transparent) could be visualized (**Fig. 14**). These results suggest the toxicity of suramin due to over dosage.

In the case of 5 µg/mL Sur-Si, on day 2, all embryos were viable with proper embryonic morphology. The optic bud formation was clear and evident. Slightly inflated embryos were observed when compared to the control group apart from which there weren't any other morphological deformities. On day 5, the embryos were analyzed for vascular deformities and blood clot. All viable embryos exhibited blood clot. Nearly 30 % embryos were dead by day 5. The remaining 70 % showed vascular deformities like blood clot, no cuverian duct formation, and reduced motility with part of the embryonic body showing opaqueness. Blood circulation in pectoral fin region was not observed (**Fig.15**). By day 9, only 40 % of embryos were viable (**Fig. 12**) of which some got hatched. The hatched larvae showed imminent deformities as bent body, blood clots at head and gill region, enlarged air bladder, low blood circulation, reduced motility etc. All these deformities can be linked to improper blood vessel formation and reduced blood circulation in the larval body. We could not observe any blood vessels in treated group on par with the control group larvae, depicting the success of vascular disruption by the suramin-loaded nanoformulation. (See Supplementary Information File and Video for data on anti-angiogenic effect of Sur-Si NPs to Medaka embryos - Analysis of morphological deformation). When the embryos were exposed to positive control agent Suramin, at a concentration of 0.05 and 0.1 mg, 90 % and 60 % of embryos remained viable.

With respect to the hatching rate of 5 µg/mL Sur-Si treated embryos (**Fig. 13**), nearly 30 % hatching was observed on day 9 whereas 10 % got hatched by day 12. This result clearly showed the negative effect of Sur-Si nanoparticles on vasculogenesis of medaka embryos. Positive controls exhibited very delayed hatching than that of Sur-Si treatment group. The 0.05 mg Suramin exposed embryos hatched by day 14 whereas all the embryos exposed to 0.1 mg Suramin hatched by day 16. The nanosize of the formulation is believed to have enhanced the accumulation of suramin into the embryos, which is otherwise an impermeable molecule, leading to telomerase

inhibition of vasculo-progenitors, and consequently affecting the formation of blood vessels. The disruption of vasculogenesis by nanoformulation in the present study led to improper blood and nutrient supply to vital organs of medaka embryos and larvae, leading to lethality or severe malformation in embryonic body or prolonged the embryonic stage, delaying the hatching. This data suggests that nanoformulation is efficient in inhibiting the neo-vascularization in medaka at the tested dose, when compared to the free drug, Suramin. The cumulative observations clearly proclaim the biocompatibility of the FITC-Si nanoparticles and their efficacy as excellent bioprobes inside an *in vivo* system and also the efficiency of the anti-angiogenic nanoformulation, Sur-Si in disrupting the process of vasculogenesis.

4. Conclusion

In this study, we successfully formulated dye or drug loaded silica nanoparticles that could be efficiently used as theranostic agents *in vitro* as well as *in vivo*. The biocompatibility and imaging potential of FITC-Si is confirmed using HuVEC cells as well as from embryonic to hatching stage of medaka. Next, we reported the anti-angiogenic potential of suramin-loaded silica to HuVEC cells, efficiently disrupting tube formation and cellular migration even under favorable conditions, and in medaka embryos, leading to either lethality or vascular disruption even at larval stage. Fluorescent nanoparticle entry into embryos was successfully demonstrated with imaging of both embryos and larvae. Apart from the intended application of the nanomaterial for imaging/therapeutic purpose, the results also open up new implications of the potent ecotoxicological aspects of the nanomaterials currently in wide practice.

5. Acknowledgement

Srivani Veeranarayanan, Aby Cheruvathoor Poulose, and M Sheikh Mohamed thank the Japanese Government's Ministry of Education, Culture, Sports, Science and Technology (MEXT) for providing financial support, as well as the Monbukagakusho fellowship. The authors thank Professor Fukushima for photoluminescence measurement assistance. Part of this study has been supported by a grant for the program of strategic research foundation at private universities S1101017, organized by the Ministry of Education, Culture, Sports, Science and Technology (MEXT), Japan since April 2012.

6. References

1. Z. Li, Q. Sun, Y. Zhu, B. Tan, Z. P. Xu, S. X. Dou, *J. Mater. Chem. B,* 2014, **2**, 2793.
2. P. Bhattacharya, D. Du, Y. Lin, *J. R. Soc. Interface,* 2014, **11,** 20131067.
3. F. Allhoff, P. Lin, D. Moore, What Is Nanotechnology And Why Does It Matter?: From Science To Ethics, 2010, *Wiley-Blackwell*, Chichester, UK.
4. A. C. Poulose, S. Veeranarayanan, M. S. Mohamed, S Raveendran, Y. Nagaoka, Y. Yoshida, T. Maekawa, D. S. Kumar, *J. Fluoresc.,* 2012, **22**, 931.
5. A. C. Poulose, S. Veeranarayanan, A. Aravind, Y. Nagaoka, Y. Yoshida, T. Maekawa, D. S. Kumar, *Materials Express,* 2012, **2**, 94.
6. S. Veeranarayanan, A. C. Poulose, M. S. Mohamed, Y. Nagaoka, S. Iwai, Y. Nakagame, S. Kashiwada, Y. Yoshida, T. Maekawa, D. S. Kumar, *Int. J. Nanomedicine,* 2012, **7**, 3769.
7. M. S. Mohamed, S. Veeranarayanan, A. C. Poulose, Y. Nagaoka, H. Minegishi, Y. Yoshida, T. Maekawa, D. S. Kumar, *Biochim. Biophys. Acta,* 2014, **1840**, 1657.
8. A. C. Poulose, S. Veeranarayanan, M. S. Mohamed, Y. Nagaoka, R. R. Aburto, T. Mitcham, P. M. Ajayan, R. R. Bouchard, Y. Sakamoto, Y. Yoshida, T. Maekawa, D. S. Kumar, *Nanoscale,* 2015, DOI: 10.1039/C4NR07139E.
9. M. S. Mohamed, S. Veeranarayanan, A. Baliyan, A. C. Poulose, Y. Nagaoka, H. Minegishi, S. Iwai, Y. Shimane, Y. Yoshida, T. Maekawa, D. S. Kumar, *Macromol. Biosci.,* 2014, **12**, 1696.
10. I. I. Slowing, J. L. Vivero-Escoto, C. W. Wu, V. S. Y. Lin. *Adv. Drug Deliv. Rev.,* 2008, **60**, 1278.
11. M. Vallet-Regi, F. Balas, D. Arcos D, *Chem Angew. Int. Ed.* 2007, **46**, 7548.
12. L. Tang, J. Cheng, *Nano Today*, 2013, **8**, 290.
13. The Royal Society and The Royal Academy of Engineering. Nanoscience and Nanotechnologies: Opportunities and Uncertainties. London, UK, 2004.
14. L. Tang, X. Yang, Q. Yin, K. Cai, H. Wang, I. Chaudhary, C. Yao, Q. Zhao. M. Kwon, J. A. Hartman, I. T. Dobrucki, L. W. Dobrucki, L. B. Borst, S. Lezmi, W. G. Helfrich, A. L. Ferguson, T. M. Fan, J. Cheng, *PNAS*, 2014, **111**, 15344.
15. H. Cabral, Y. Matsumoto, L. Mizuno, Q. Chen, M. Murakami, M. Kimura, Y. Terada, M. R. Kano, K. Miyazono, M. Uesaka, N. Nishiyama, K. Katoaka, *Nat. Nanotechnol.,* 2011, **6**, 815.
16. S. Huang, K. Shao, Y. Kuang, Y. Liu, J. Li, S. An, Y. Guo, H. Ma, X. He, C. Jiang, *Biomaterials,* 2013, **21**, 5294.
17. X. Zhao, L. Liu, X. Li, J. Zeng, X. Jia, P. Liu, *Langmuir,* 2014, **30**, 10419.
18. J. Folkman, *N. Engl. J. Med.,* 1971, **285**, 1182.
19. S. Gout, J. Huot, *Cancer Microenviron.,* 2008, **1**, 69.
20. J. A. Sipos, M. H. Shah, *Ther. Adv. Med. Oncol.,* 2010, **2**, 3.
21. M. Bisht, D. C. Dhasmana, S. S. Bist, *Indian J. Pharmacol.,* 2010, **42**, 2.
22. Q. Hu, X. Gao, T. Kang, X. Feng, D. Jiang, Y. Tu, Q. Song, L. Yao, X. Jiang, H. Chen, J. Chen, *Biomaterials,* 2013, **37**, 9496.
23. P. M. Winter, S. D. Caruthers, H. Zhang, T. A. Williams, S. A. Wickline, G. M. Lanza, *JACC: Cardiovascuar Imaging,* 2008, **1**, 624.
24. S. Veeranarayanan, A. C. Poulose, M. S. Mohamed, S. H. Varghese, Y. Nagaoka, Y. Yoshida, T. Maekawa, D. S. Kumar, *Small,* 2012, **8**, 3476.

25. G. N. Serbedzila, E. Flynn, C. E. Willett, *Angiogenesis,* 1999, **3**, 353.
26. M. Fujita, S. Isogai, A. Kudo, *Dev. Dyn.,* 2006, **235**, 734.
27. T. Sugise, Y. Hayashida, T. Hanafusa, E. Nanjo, I. Yamashita, *Environ. Sci. Technol.,* 2006, **40**, 2051.
28. K. Naruse, M. Tanaka, H. Takeda, Medaka: A Model for Organogenesis, Human Disease, and Evolution, 2011, Springer Science & Business Media.
29. S. Veeranarayanan, A. C. Poulose, M. S. Mohamed, A. Aravind, Y. Nagaoka, Y. Yoshida, T. Maekawa, D. S. Kumar, *J. Fluoresc.,* 2012, **22**, 537.
30. C. Barbe, J. Bartlett, L. G. Kong, K. Finnie, H. Q. Lin, M. Larkin, S. Calleja, A. Bush, G. Calleja, *Adv. Mater.,* 2004, **16**, 1959.

FIGURES

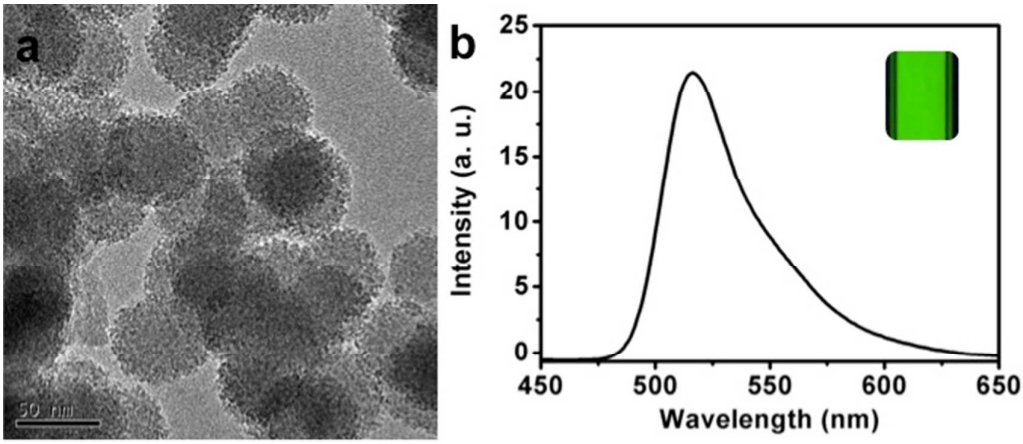

Figure 1: *a) TEM image of Si NPs and b) Photoluminescence of FITC-Si NPs. The inset in b) shows the fluorescence of the FITC-Si NPs under UV excitation.*

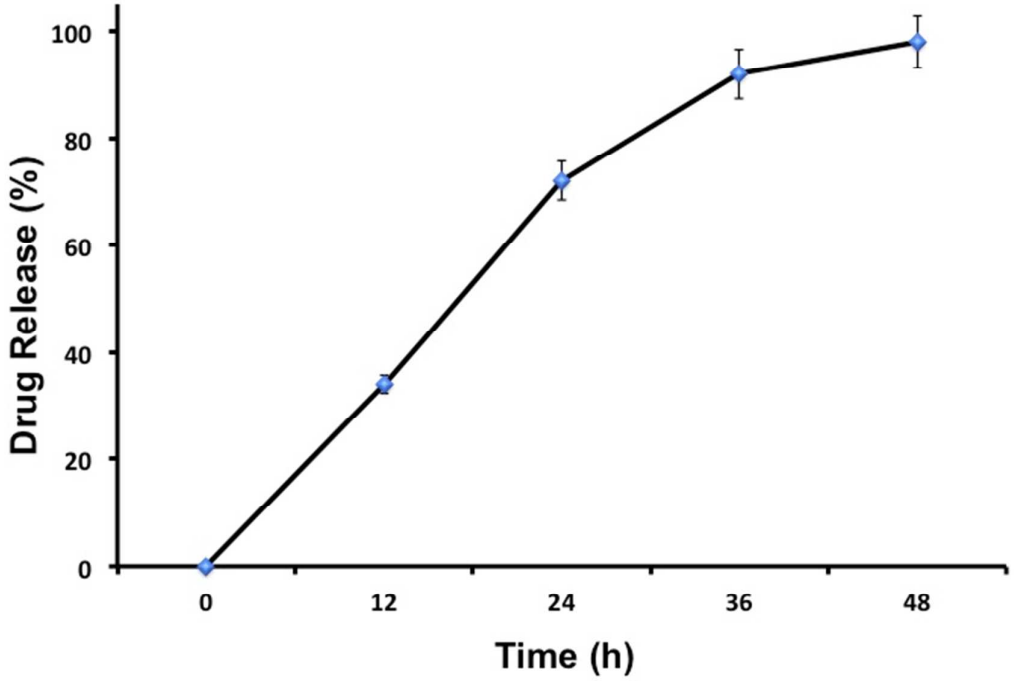

Figure 2: *Release of Suramin from Sur-Si NPs. The release was measured at pH 7.4.*

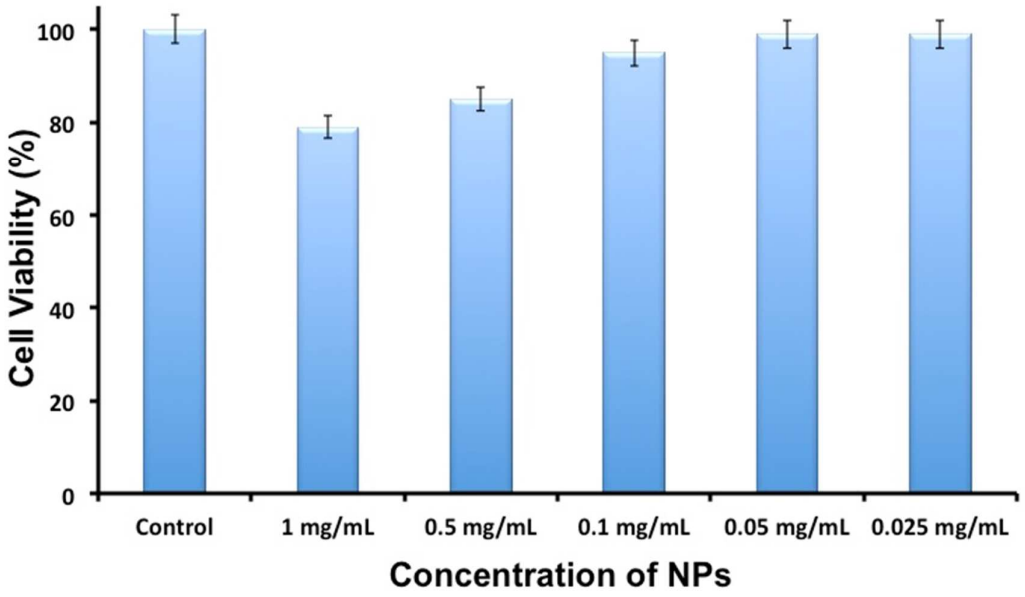

Figure 3: *Biocompatibility of FITC-Si NPs in HuVEC cells. Different concentration of FITC-Si NPs (0.025 – 1 mg/mL) was exposed to the cells for 72 h, post that the viability is read using Alamar blue assay.*

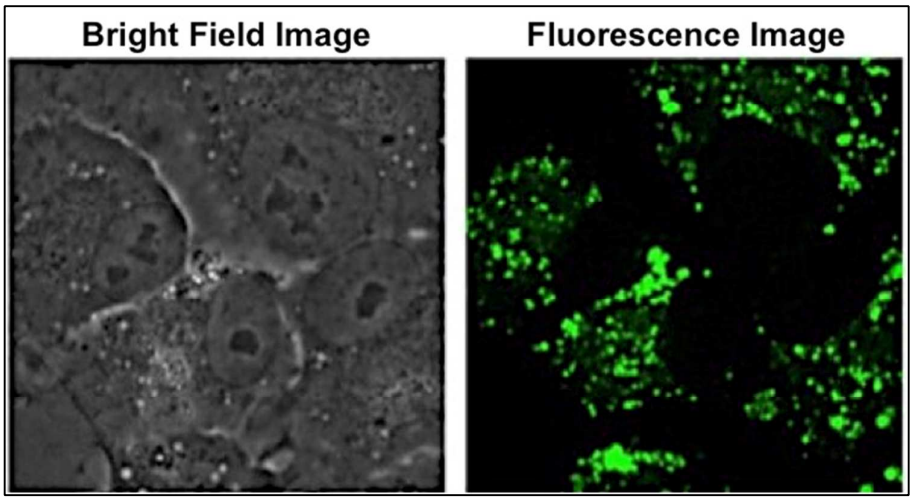

Figure 4: *Confocal bright field and fluorescence image of FITC-Si NPs exposed HuVEC cells. The fluorescence imaging was carried out using 488 nm as excitation wavelength.*

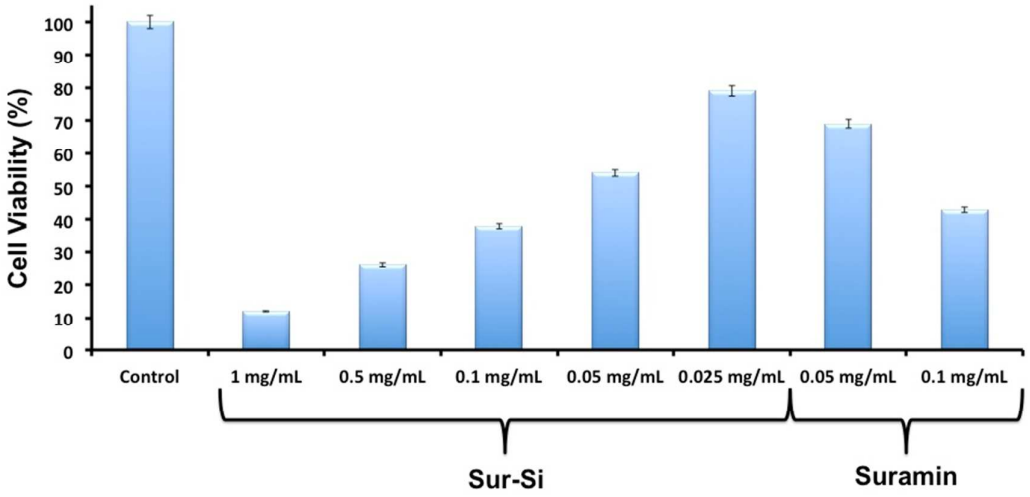

Figure 5: *In vitro cytotoxicity of Sur-Si NPs. Different concentration of Sur-Si NPs (0.025 – 1 mg/mL) and Suramin (0.05 – 0.1 mg/mL) were exposed to the cells for 72 h, post that the viability is read using Alamar blue assay.*

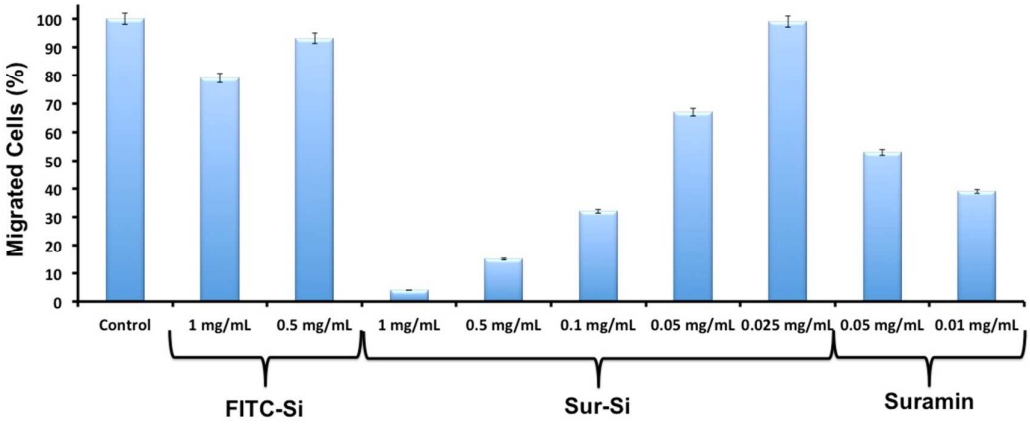

Figure 6: *Analysis of HuVECs migratory potential in presence of Sur-Si NPs. Different concentration FITC-Si and Sur-Si NPs (0.025 – 1 mg/mL) and Suramin (0.05 – 0.1 mg/mL) was exposed to the cells for 24 h, post that the migrated cell population was quantified with trypan blue.*

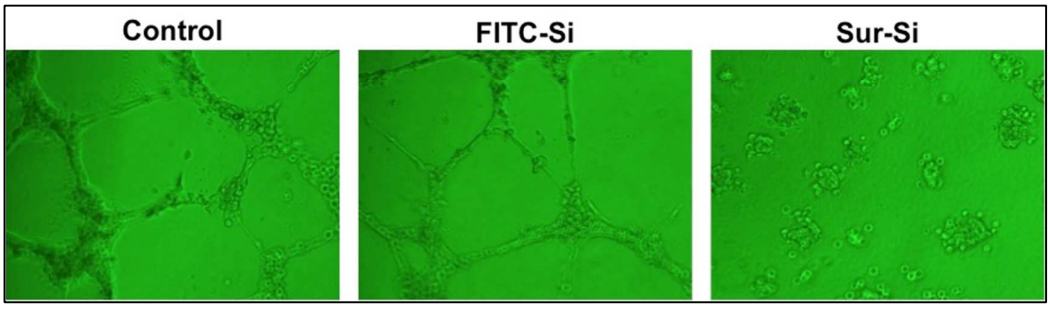

Figure 7: *Analysis of HuVECs tubulogenesis ability in presence of Sur-Si NPs. FITC-Si and Sur-Si NPs were exposed to the cells for 4 h, post that the tubulogenesis was photographed with phase contrast microscope.*

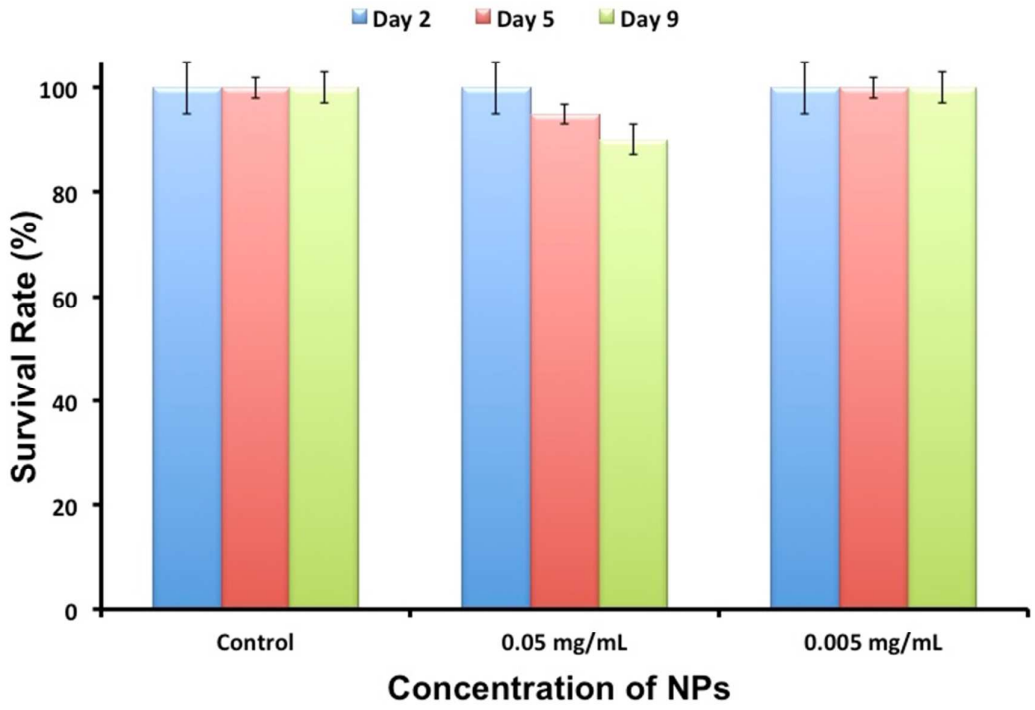

Figure 8: *Survival rate of medaka embryos exposed to FITC-Si NPs (at 0.05 and 0.005 mg/mL concentration).*

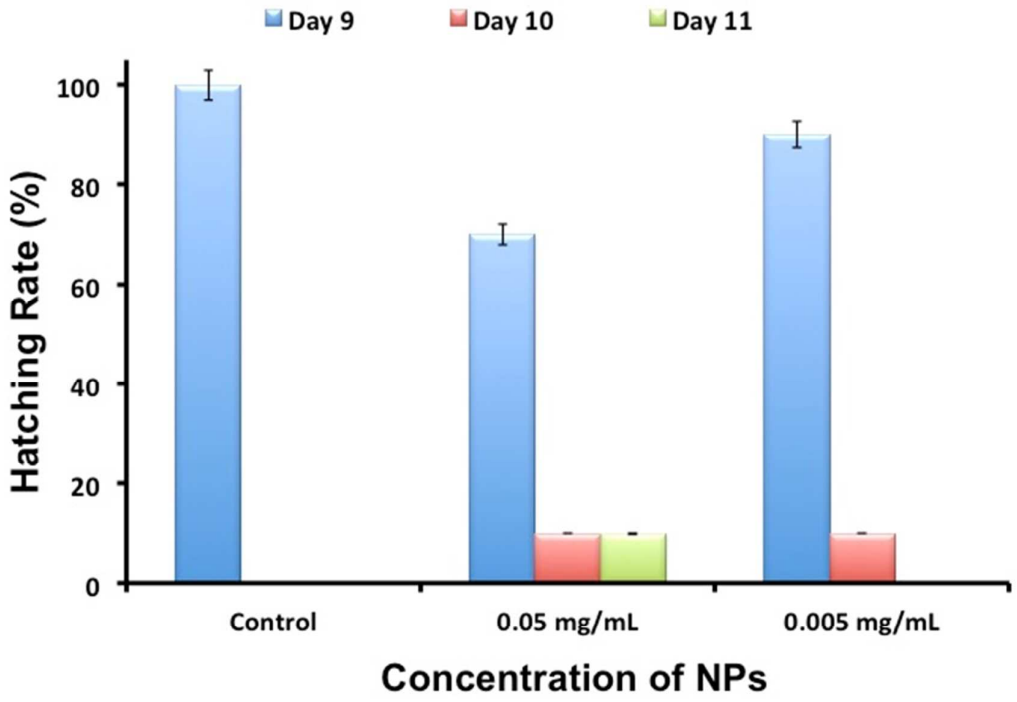

Figure 9: *Hatching rate of medaka embryos exposed to FITC-Si NPs (at 0.05 and 0.005 mg/mL concentration).*

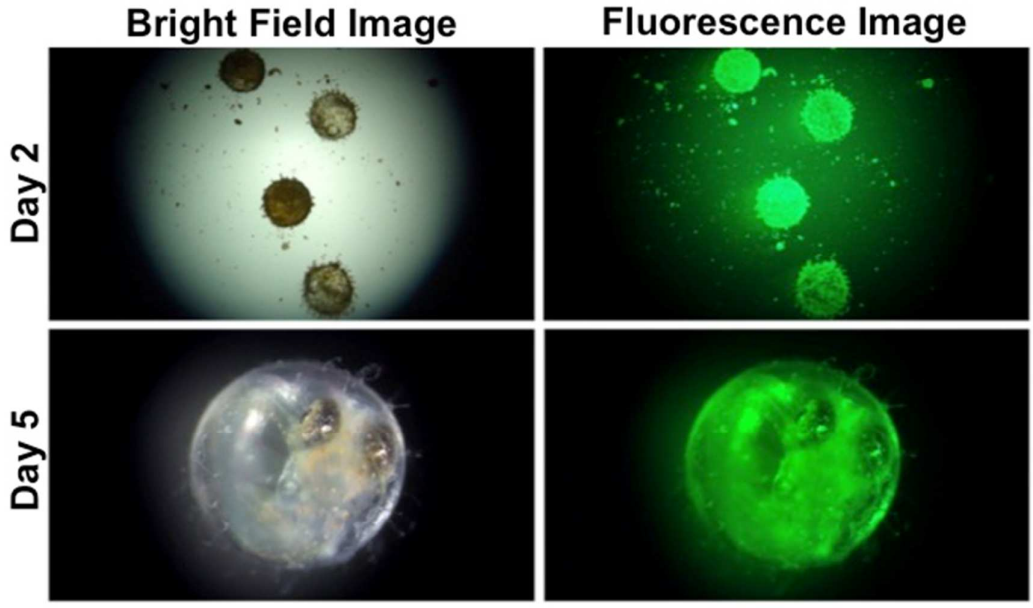

Figure 10: *Imaging of medaka embryos exposed to FITC-Si NPs at 0.05 mg/mL concentration on Day 2 and 5.*

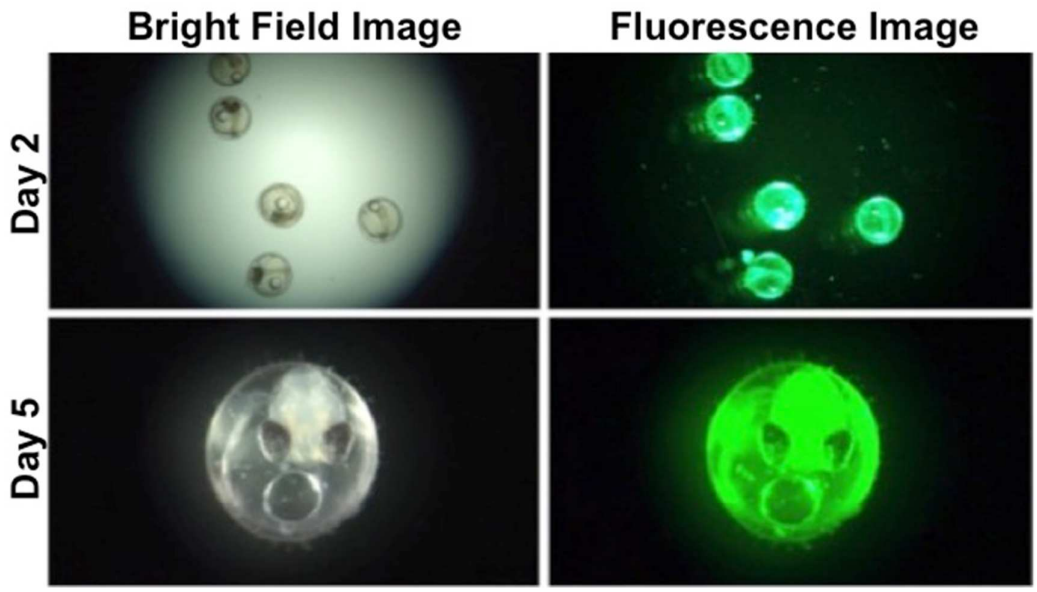

Figure 11: *Imaging of medaka embryos exposed to FITC-Si NPs at 0.005 mg/mL concentration on Day 2 and 5.*

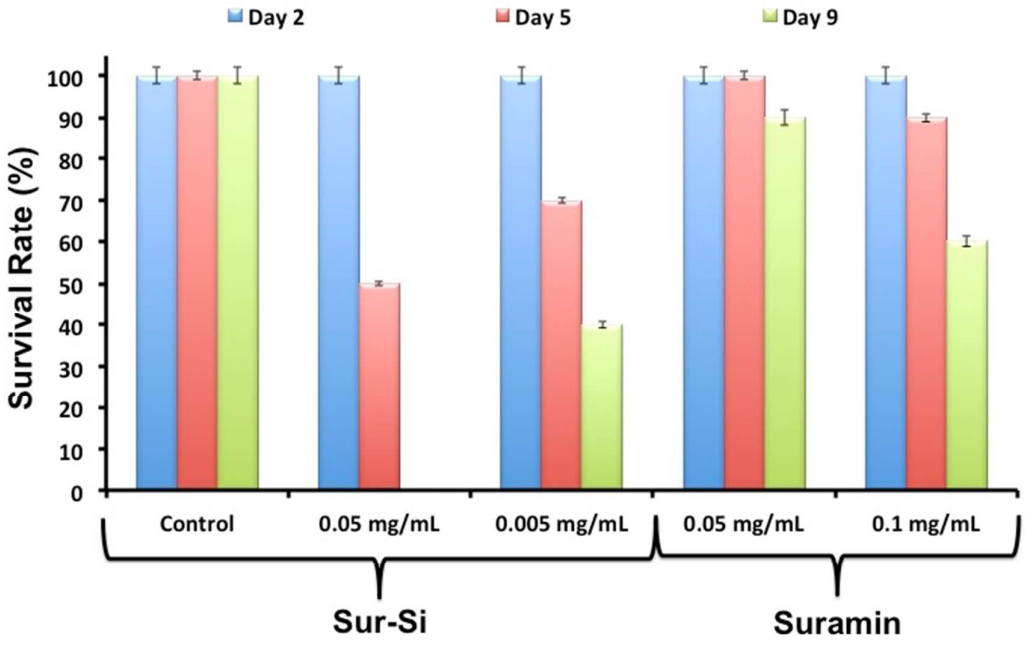

Figure 12: *Survival rate of medaka embryos exposed to Sur-Si NPs (at 0.05 and 0.005 mg/mL concentration). Suramin (0.05 – 0.1 mg/mL) was used as positive control agent.*

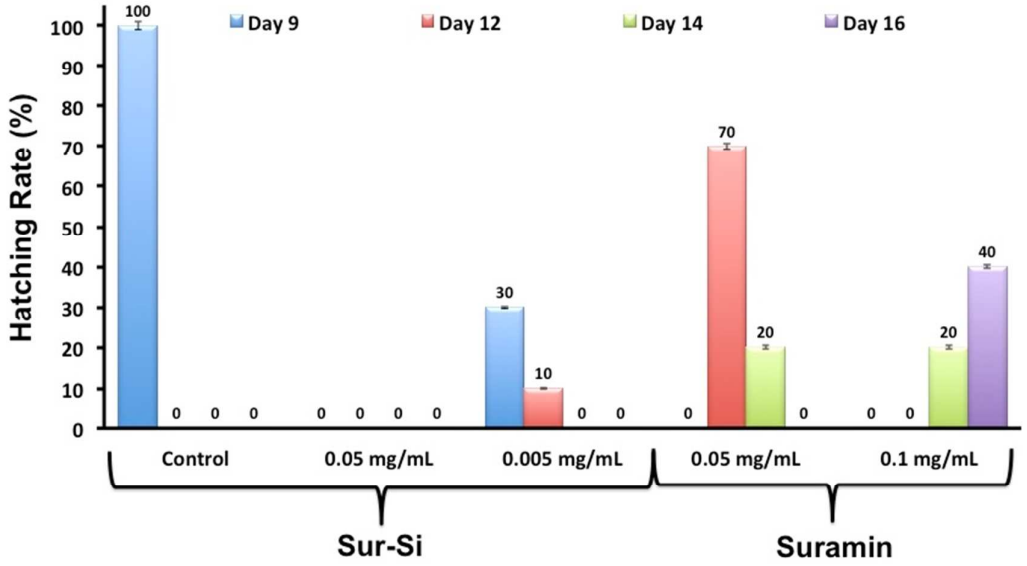

Figure 13: *Hatching rate of medaka embryos exposed to Sur-Si NPs (at 0.05 and 0.005 mg/mL concentration). Suramin (0.05 – 0.1 mg/mL) was used as positive control agent.*

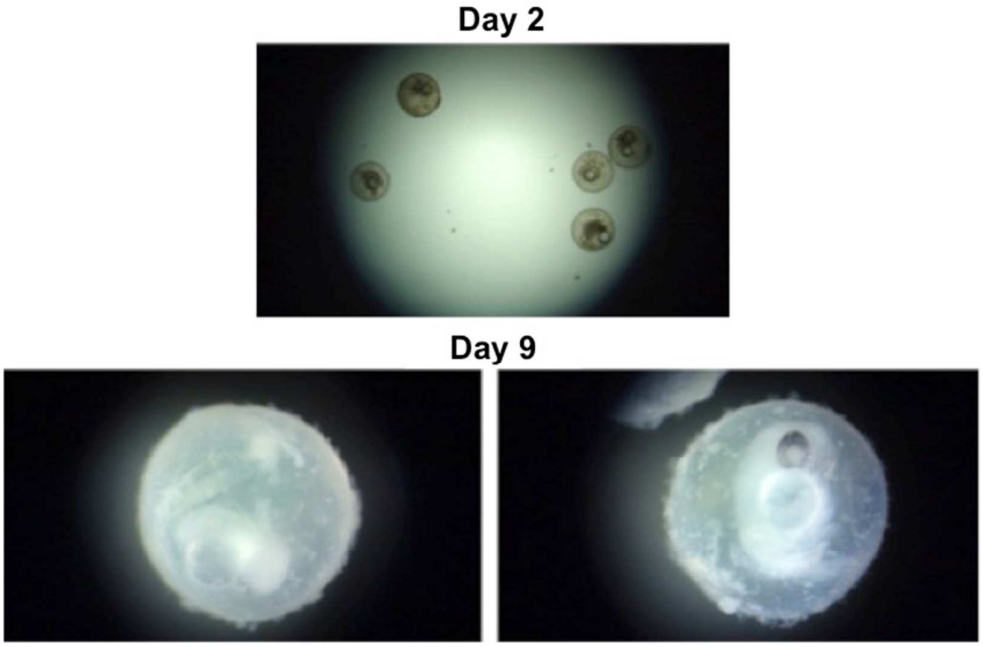

Figure 14: *Bright field images of medaka embryos exposed to Sur-Si NPs at 0.05 mg/mL concentration on Day 2 and 9.*

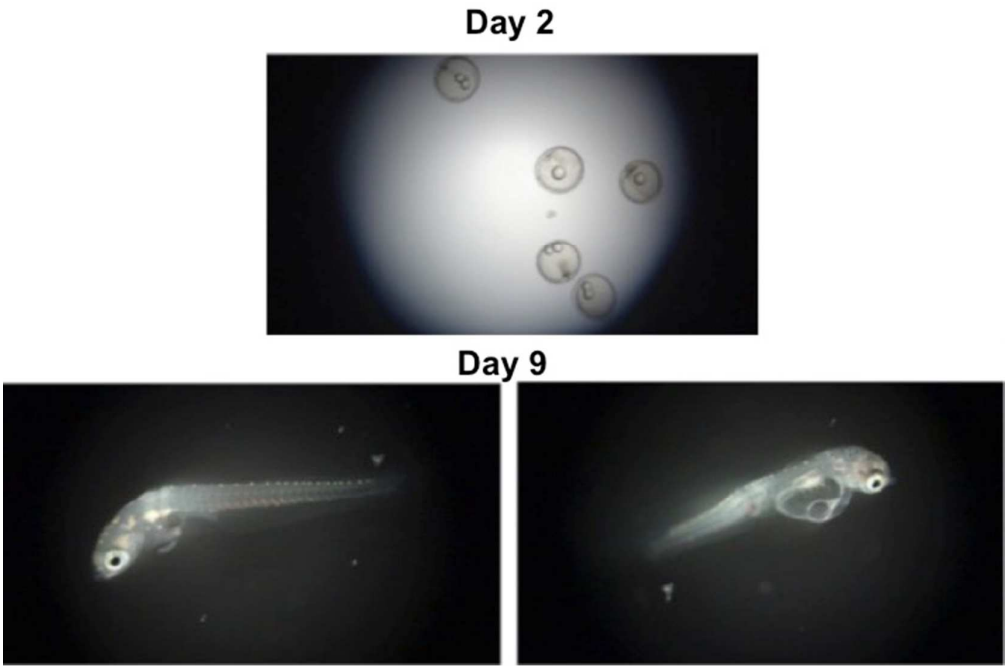

Figure 15: *Bright field images of medaka embryos exposed to Sur-Si NPs at 0.005 mg/mL concentration on Day 2 and 9.*

GRAPHICAL ABSTRACT

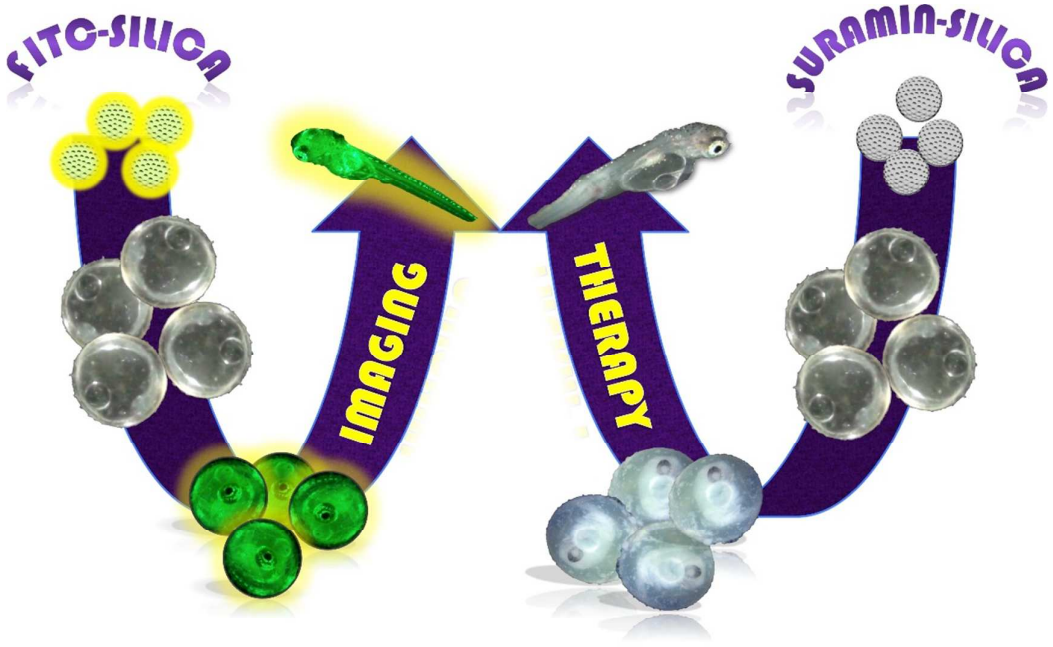

A silica based nanoformulation for imaging cum anti-angiogenic therapy of is reported. The nanoformulation is tested for its efficacy to perform live embryo/larvae imaging post exposure to fresh embryos. The vascular disruption and its related morphological deformities in medaka embryos/larvae, due to exposure to anti-angiogenic nanoformulation depicts the use of this nanoformulation for future combinatorial/alternative anti-angiogenic cancer theranostics.